

# A TECHNIQUE FOR FOREGROUND SUBTRACTION IN REDSHIFTED 21 CM OBSERVATIONS

JUNGYEON CHO<sup>1</sup>, A. LAZARIAN<sup>2</sup>, AND PETER T. TIMBIE<sup>3</sup>

*Draft version July 16, 2018*

## ABSTRACT

One of the main challenges for future 21 cm observations is to remove foregrounds which are several orders of magnitude more intense than the HI signal. We propose a new technique for removing foregrounds of the redshifted 21 cm observations. We consider multi-frequency interferometer observations. We assume that the 21 cm signals in different frequency channels are uncorrelated and the foreground signals change slowly as a function of frequency. When we add the visibilities of all channels, the foreground signals increase roughly by a factor of  $\sim N$  because they are highly correlated. However, the 21 cm signals increase by a factor of  $\sim \sqrt{N}$  because the signals in different channels contribute randomly. This enables us to obtain an accurate shape of the foreground angular power spectrum. Then, we obtain the 21-cm power spectrum by subtracting the foreground power spectrum obtained this way. We describe how to obtain the average power spectrum of the 21 cm signal.

*Subject headings:* cosmology: observations—cosmology: large-scale structure of universe —ISM: general—turbulence

## 1. INTRODUCTION

A promising emerging field in cosmology is the proposed use of 21-cm emission from neutral hydrogen to trace the evolution of structure in the universe from redshift 0 to 50. At redshifts up to about 3, by mapping the three-dimensional intensity field with 10 arc-minute resolution, it may be possible to precisely measure the expansion history throughout the transition from deceleration to acceleration (Chang et al. 2008; Wyithe et al. 2008; Loeb & Wyithe 2008; Morales & Wyithe 2010). For redshifts near 10 several instruments are under construction to search for 21-cm emission from the Epoch of Reionization (EoR; Morales & Hewitt 2004; Zaroubi & Silk 2005; Backer et al. 2007). Some authors even suggest that observations at redshifts well above 10 may provide very sharp tests of the world model and the composition of the cosmic fluid (Loeb & Zaldarriaga 2004).

Most of the observational effort so far has focused on searching for the EoR signal. The first goal of current EoR programs is to pin down the redshift of reionization. Later measurements will address questions such as the following: What were the first sources of ionizing radiation? What is the power spectrum of the HI structure, and how did it evolve? The first generation of 21-cm EoR observatories may begin to attack this last question by observing the emission of the neutral hydrogen itself. The interpretation of the data in terms of pinning down the UV sources is likely to be much more difficult.

Even at the end of the EoR, there is still enough HI (a few percent of all the hydrogen) in the form of self-shielded clumps to be visible at a brightness temperature contrast of  $\Delta T \sim 1$  mK. We have some information about these structures since they are seen via UV absorption as Damped Lyman Alpha regions, or DLA's

(Wolfe et al. 2005). Observation of 21-cm fluctuations from such systems provides a tool for understanding structure formation in the post-reionization era. These HI regions presumably trace the dark matter and hence can be used to study the evolution of the matter power spectrum. Measurement of the cosmic power spectrum as a function of redshift over the cosmic volume  $0.5 < z < 6$  could provide cosmic-variance limited determination of cosmological parameters such as the equation of state of the dark energy and the neutrino mass (Loeb & Wyithe 2008).

Multiple lines of observational evidence now indicate that dark energy accounts for  $\sim 70\%$  of the energy density in the universe, but so far we have few clues as to the physics underlying this phenomenon. There are a host of dark energy models and these can be distinguished by their equations of state. A promising approach is to infer the equation of state from the distance-redshift relation in the redshift range of 0 to about 2. In particular, baryon-acoustic oscillations (BAO) can provide a standard ruler for distance determinations. The BAO ‘wiggles’ in the matter power spectrum can be measured efficiently using 21-cm intensity mapping (Chang et al. 2008; Ansari et al. 2008, 2011; Seo et al. 2010)

To achieve these scientific goals a wide variety of innovative 21-cm telescope designs have been proposed, some prototypes built, and some telescopes completed (see Morales & Wyithe 2010, for a review of these instruments and their scientific potential). However, there are many development tasks needed to advance the state of the art of 21-cm cosmology, including calibration strategies, low-noise amplifier development, correlator design, examination of array layouts, radio-quiet site development, and foreground removal.

One of the main difficulties of all 21-cm telescopes is to remove foregrounds which are several orders of magnitude more intense than the HI signal (Morales et al. 2006). The basic idea is that most foregrounds have a smooth power-law frequency dependence in contrast with the HI signal. The exception is Galactic radio

<sup>1</sup> Dept. of Astronomy and Space Science, Chungnam National University, Daejeon, Korea

<sup>2</sup> Dept. of Astronomy, University of Wisconsin, Madison, WI 53706, USA

<sup>3</sup> Dept. of Physics, University of Wisconsin, Madison, WI 53706, USA

recombination lines which occur at known frequencies and can be excised. The main foregrounds are the Galactic synchrotron radiation and extragalactic point sources. Other sources like free-free electron emission (*i.e.* Bremsstrahlung) are much less intense and have power-law spectra similar to the first two components.

Other foreground removal techniques have been proposed as well. Morales *et al.* (2006) review these techniques and show how to correct the errors they cause in the recovered power spectrum. Liu *et al.* (2009) show that performing foreground removal in Fourier space eliminates errors that arise from frequency-dependent beam patterns (mode mixing). Liu *et al.* (2011) have developed a technique for estimating the power spectrum in the presence of foregrounds without introducing noise or bias to the power spectrum.

Simulations by Bowman, Morales and Hewitt (2009) for the Murchison Widefield Array remove the contribution from bright identified sources and then in each RA-dec pixel fit and subtract a polynomial in  $\nu$ . This two-step strategy allows for the observation of the HI signal at the time of reionization ( $z \approx 8$ ). Similar foreground removal simulations have been applied to candidate dark energy observatories; Ansari *et al.* 2011 show how foregrounds might be separated from the HI signal based on their differing spectral signatures as measured by an interferometric array of dishes or cylinder telescopes.

Below we discuss a different idea for removing foregrounds which is based on using the power spectrum. The physical basis of the idea is that at different frequencies the fluctuations of redshifted HI are not correlated, as we sample completely different regions of HI, while the foreground fluctuations are correlated as they arise from the same galactic inhomogeneities, *e.g.* turbulent fluctuations as discussed in Cho & Lazarian 2002; 2010. However, unlike Cho & Lazarian (2010) the suggested analysis does not require assumptions about the power spectrum of fluctuations.

In §2 we discuss the technique that we propose, in §3 the applicability of our technique, and in §4 we summarize our results.

## 2. METHOD

### 2.1. Assumptions

We assume the following:

1. The observations are made at  $N$  different frequency channels ( $\nu_i$ ,  $i=1, \dots, N$ ) and data are collected in  $uv$  coordinates. We assume that  $\delta\nu$  ( $\equiv \nu_{i+1} - \nu_i$ ) is constant. We denote the visibility at channel  $i$  as  $T_{\nu_i}(u, v)$ .
2. Observations are made for a small patch on the sky. We use  $(\theta_x, \theta_y)$  to denote a position on the sky plane. We use either  $(k_x, k_y)$  or  $(u, v)$  to denote a position in Fourier space. Note that  $l = 2\pi(u^2 + v^2)^{1/2}$  (White et al. 1999) and  $C_l^{\nu_i} \propto |T_{\nu_i}(u, v)|^2 = (1/N_{sum}) \sum_{l/2\pi} |T_{\nu_i}(u, v)|^2$ , where the summation is done for  $(l/2\pi) \leq \sqrt{u^2 + v^2} < (l/2\pi) + (\Delta l/2\pi)$  and  $N_{sum}$  is the number of modes used for the summation.
3. The 21-cm signals from different frequency channels are uncorrelated.

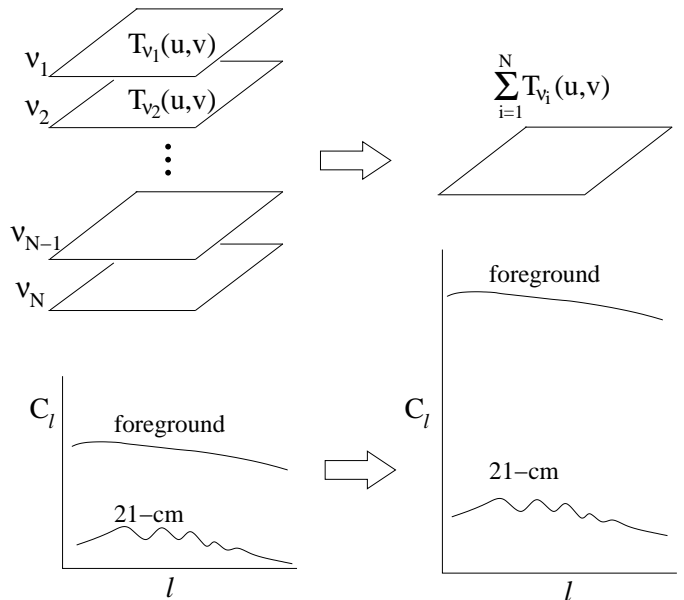


FIG. 1.— Method. *Left*: Observations are done in  $N$  different frequency channels ( $\nu = \nu_1, \dots, \nu_N$ ). The foreground signals are several orders of magnitude stronger than the 21-cm signal (low-left panel). We assume that the 21-cm signals from different channels are uncorrelated. However, we assume the foreground signals from different channels are highly correlated. *Right*: When we add all  $T_{\nu_i}(u, v)$ 's, the foreground signals are enhanced by a factor of  $\sim N$ , while the 21-cm signal is enhanced by a factor of  $\sim \sqrt{N}$ . In terms of angular spectrum, the foreground spectrum goes up by a factor of  $\sim N^2$  and the 21-cm spectrum goes up by  $\sim N$ . The angular spectrum of  $T_{avg}(u, v) \equiv \sum_i T_{\nu_i}(u, v)/N$  will be  $\sim C_l^{for} + C_l^{21cm}/N$ , where 'for' and '21-cm' stand for the foreground and the redshifted 21-cm, respectively. Therefore, the spectrum of  $T_{avg}(u, v)$ ,  $C_l^{avg}$ , should represent an accurate shape of the foreground spectrum. We can obtain the 21-cm spectrum by subtracting the foreground spectrum.

4. The cross-correlation between the foreground and the 21-cm signals is negligible. This is not a trivial issue if the 21-cm signal is much weaker than the foreground one. We will come back to this in §3.
5. The noise level is lower than the 21-cm signal. See also discussions in §3.

### 2.2. Basic idea

We can obtain an accurate shape of the foreground angular power spectrum in the following way. Suppose that we have multi-channel observation data in  $uv$  coordinates (left panel of Fig. 1). We stack all the  $uv$  plane data into a single file (right panel of Fig. 1). That is, we calculate  $\sum_{i=1}^N T_{\nu_i}(u, v)$ . (If the observations are done in real space, we first obtain  $\sum_{i=1}^N T_{\nu_i}(\theta_x, \theta_y)$  and then we perform a Fourier transform.) In the stacked map, since the foreground signals in different channels are correlated, they are enhanced by a factor of  $\sim N$ . However, the noise and the 21-cm signals are enhanced by a factor of  $\sqrt{N}$  because they contribute randomly. Therefore, the contrast between the foreground and the noise/21-cm angular spectra will be increased by  $\sim N$  times. In this way we can obtain an accurate shape of the foreground power spectrum. We define  $T_{avg}(u, v)$  as

$$T_{avg}(u, v) \equiv \frac{1}{N} \sum_{i=1}^N T_{\nu_i}(u, v). \quad (1)$$

What, then, does  $T_{avg}(u, v)$  mean? If  $T_{\nu}(u, v)$  varies slowly as a function of  $\nu$ , we can show that the obtained foreground power spectrum is a good representation for the power spectrum at the central channel ( $\nu = \nu_{(N+1)/2}$ ). Suppose that  $N$  is an *odd* number. Then we can write

$$T_{\nu_i}^{for}(u, v) = T_{\nu_{(N+1)/2}}^{for}(u, v) + a\Delta\nu, \quad (2)$$

where  $a$  is a constant,  $\Delta\nu = \nu_i - \nu_{(N+1)/2}$  and the superscript ‘for’ denotes the foreground. We assume  $|a\Delta\nu| \ll |T_{\nu_i}^{for}|$  and we ignore the second-order quantities. From Eqs. (1) and (2), we have  $\frac{1}{N} \sum_{i=1}^N T_{\nu_i}(u, v) \approx T_{\nu_{(N+1)/2}}^{for}(u, v)$ , which results in

$$C_l^{avg} \approx C_l^{\nu_{(N+1)/2}, for}, \quad (3)$$

where  $C_l^{avg}$  and  $C_l^{\nu_i, for}$  are the angular power spectra of  $T_{avg}(u, v)$  and  $T_{\nu_i}^{for}(u, v)$ , respectively.

The foreground power spectrum ( $\approx C_l^{avg}$ ), as well as the foreground map ( $\approx T_{avg}(u, v)$ ), can be used for other observations. For example, when a future low-noise single channel observation becomes available at  $\nu = \nu_{(N+1)/2}$ , we can use  $C_l^{avg}$  or  $T_{avg}(u, v)$  to subtract the foreground. It is also possible to use them for future high angular resolution low-noise observations. Cho & Lazarian (2010) argued that when accurate foreground observations are available for a certain range of  $l$ ’s, we can extrapolate the foreground spectrum to a range of  $l$  where no foreground information is available. Therefore, if a very high angular resolution single-frequency observation is performed in the future, we can extrapolate the foreground spectrum (i.e.  $C_l^{avg}$ ) to higher values of  $l$  and extract the 21-cm information on the small scales.

### 2.3. Proposed techniques

**Case 1: same power spectrum shape for all channels**—In this case, we can easily obtain  $C_l^{\nu_i, 21cm}$ . Note that, at this moment, we know only the shape (the  $l$ -dependence) of  $C_l^{\nu_i, for}$ . The amplitude can be different in each frequency channel and we do not know it yet. We can determine the amplitude by fitting or by the following method. Suppose that the value of

$$\sum_l |\log(C_l^{\nu_i}) - \log(\alpha C_l^{avg})|^2 \quad (4)$$

has a minimum value at  $\alpha = \alpha_i$ . Then we have

$$C_l^{\nu_i, 21cm} \approx C_l^{\nu_i} - \alpha_i C_l^{avg}. \quad (5)$$

**Case 2: linear dependence of  $\mathbf{T}(u, v)$  on  $\nu$** —In this case, as we discussed in the previous subsection, we have  $C_l^{avg} = C_l^{\nu_{(N+1)/2}, for}$ . The 21-cm spectrum at  $\nu = \nu_i$  is

$$C_l^{\nu_i, 21cm} = C_l^{\nu_i} - C_l^{\nu_i, for}. \quad (6)$$

From Eq. (2), we have

$$C_l^{\nu_i, for} = C_l^{\nu_{(N+1)/2}, for} + A\Delta\nu, \quad (7)$$

where  $A = Re[2 \sum_{l/2\pi} T_{\nu_{(N+1)/2}}^{for}(u, v) a^*]$ . Here ‘\*’ denotes the complex conjugate and  $Re[...]$  stands for the

real part. Therefore, the average spectrum of the 21-cm signal over  $N$  channels is

$$\frac{1}{N} \sum_{i=1}^N C_l^{\nu_i, 21cm} = \frac{1}{N} \left( \sum_{i=1}^N C_l^{\nu_i} \right) - C_l^{avg}. \quad (8)$$

**Case 3: quadratic dependence of  $\mathbf{T}(u, v)$  on  $\nu$** —In this more general case, we can obtain the average 21-cm spectrum. Suppose that  $N = \text{even}$  for simplicity. Then we can write

$$T_{\nu_i}^{for}(u, v) = f_0 + a\Delta\nu + b\Delta\nu^2, \quad (9)$$

where  $f_0$  is a visibility at  $\nu_0 = (\nu_{N/2} + \nu_{1+N/2})/2$  (not observed),  $a$  and  $b$  are constants,  $\Delta\nu = \nu_i - \nu_0 = [i - (N+1)/2]\delta\nu$ , and  $\delta\nu = \nu_{i+1} - \nu_i$ . We note that

$$\begin{aligned} |T_{avg}(u, v)|^2 &= \left| f_0 + \frac{b}{2N} \Delta\nu_0^2 \sum_{j=1}^{N/2} (2j-1)^2 \right|^2, \\ &= |f_0|^2 + \frac{1}{N} \Delta\nu_0^2 \sum_{j=1}^{N/2} (2j-1)^2 Re[f_0 b^*]. \end{aligned} \quad (10)$$

On the other hand, we have

$$\begin{aligned} &\sum_{i=1}^{N/2} |T_{\nu_i}(u, v) + T_{\nu_{N-i+1}}(u, v)|^2 \quad (11) \\ &= \sum_{j=1}^{N/2} \left| 2f_0 + \frac{b}{2} (2j-1)^2 \delta\nu^2 \right|^2 + \sum_{i=1}^{N/2} |T_{\nu_i}^{21cm} + T_{\nu_{N-i+1}}^{21cm}|^2 \\ &= 2N|f_0|^2 + 2\delta\nu^2 \sum_{j=1}^{N/2} (2j+1)^2 Re[f_0 b^*] + \sum_{i=1}^N |T_{\nu_i}^{21cm}|^2 \end{aligned}$$

where we dropped the cross-correlation terms between the 21-cm and the foreground signals (see §3). If we subtract Eq. (10) times  $2N$  from Eq. (11), we have  $\sum_{i=1}^N |T_{\nu_i}^{21cm}|^2$ . Therefore, the average spectrum of the 21-cm signal is

$$\frac{1}{N} \sum_{i=1}^N C_l^{\nu_i, 21cm} = \frac{1}{N} \left( \sum_{i=1}^N D_l^{\nu_i} \right) - 2C_l^{avg}, \quad (12)$$

where  $D_l^{\nu_i}$  is the angular spectrum of  $T_{\nu_i}(u, v) + T_{\nu_{N-i+1}}(u, v)$ <sup>4</sup>.

### 3. DISCUSSION

Our technique critically depends on the assumption of slow variation of the  $T_{\nu_i}^{for}(u, v)$  over frequency channels. This assumption may need further investigation. However, we believe that this is a good assumption due to the following reasons. First of all, we know that the major foreground, which is the synchrotron foreground, is caused by MHD turbulence (see the statistical description of fluctuations in Lazarian & Pogosyan 2012). The variations with frequency from an elementary synchrotron emitting volume are given by  $\propto n_0 B_{\perp}^2 \nu^{(1-\alpha)/2}$

<sup>4</sup> More precisely, the right hand side is multiplied by  $N/(N-2)$ . Similarly, the right hand side of Eq. (8) is multiplied by  $N/(N-1)$ .

where  $B_{\perp}$  is the magnetic field strength perpendicular to the line of sight and the number density of cosmic rays has a power law distribution  $n(E)dE = n_0 E^{-\alpha} dE \sim n_0 E^{-3} dE$ . Therefore we expect the spectral components to change as  $\propto (\nu/\nu_0)^{-1}$ . This dependence can be compensated over the frequency interval of  $\Delta\nu = (N-1)\delta\nu$  and the residual emission, e.g. arising from other subdominant components of the foreground, may be treated with the suggested technique. The dependence of the other foreground components, e.g. free-free, dust and spinning dust (see Lazarian & Finkbeiner 2003, for a review) on the frequency is weak and therefore the linear/quadratic expansion in frequencies in Eq. (2)/(9) should be also valid. If we observe, for example, 610 MHz, the 21-cm signal is believed to be decorrelated if  $\Delta\nu > 0.5$  MHz (see for example Ghosh et al. 2011). If we use 12 channels, we have  $\Delta\nu/\nu_0 = 5.5/610 \approx 0.01$ . Therefore, any third or higher order effects should be very small. For synchrotron, since  $(\nu/\nu_0)^{-1} = \sum_{n=0}^{\infty} (1 - \nu/\nu_0)^n$ , the ratio of the third to the second term of the expansion is  $\sim O(\nu/\nu_0 - 1) \sim 0.01$ . For free-free the frequency dependence is weaker and truncation error will be smaller.

In this paper we assume that the cross-correlation between the foreground and the 21-cm signals is negligible. This needs further verification. In general, we can write  $C_l = C_l^{for} + C_l^{21cm} + C_l^{cc}$ , where

$$C_l^{cc} = Re \left[ \frac{2}{N_{sum}} \sum_{l/2\pi} T^{for}(u, v) T^{21cm}(u, v)^* \right] \quad (13)$$

is the cross-correlation term. When the 21-cm signal is  $\gamma$  times smaller than the foreground one (i.e.  $T^{21cm} \sim T^{for}/\gamma$ ), the cross-correlation term  $C_l^{cc}$  can be larger than  $C_l^{21cm}$  if the number of modes used for the summation in Eq. (13) is less than  $\sim \gamma^2$ .

However, if we use Eq. (12) or (8), we may circumvent this difficulty. Let us consider the more general case of Eq. (12). The cross-correlation term that will appear additionally in the right-hand side of Eq. (12) is

$$C_l^{cc} = Re \left[ \frac{2}{N_{sum}} \sum_{l/2\pi} (\mathcal{A} - \mathcal{B}) \right], \quad (14)$$

$$\mathcal{A} = \frac{1}{N} \sum_{i=1}^{N/2} \left[ (2f_0 + 2b\Delta\nu^2) (T_{\nu_i}^{21cm} + T_{\nu_{N-i+1}}^{21cm})^* \right], \quad (15)$$

$$\mathcal{B} = \frac{2}{N^2} \left( \sum_{i=1}^N (f_0 + b\Delta\nu^2) \right) \left( \sum_{i=1}^N T_{\nu_i}^{21cm*} \right), \quad (16)$$

$$|\mathcal{A} - \mathcal{B}| \lesssim 2|b|\Delta\nu_{max}^2 |T_{\nu_i}^{21cm}| / \sqrt{N}, \quad (17)$$

where the variables are defined similarly (i.e.  $\Delta\nu = \nu_i - \nu_0$ ,  $N=\text{even}, \dots$ ), ‘ $\mathcal{A}$ ’ and ‘ $\mathcal{B}$ ’ are from the first and the second terms on the right-hand side of Eq. (12), respectively,  $\Delta\nu_{max} = \nu_N - \nu_0$ , and we dropped ‘(u,v)’ for simplicity. Note that the terms containing  $f_0$  cancel out. Therefore, if

$$2b\Delta\nu_{max}^2 / \sqrt{NN_{sum}} < |T_{\nu_i}^{21cm}|, \quad (18)$$

we can neglect the cross-correlation term. If the cross-

correlation term is indeed larger than the 21-cm spectrum  $C_l^{21cm}$  for any reason, our technique can reveal the cross-correlation spectrum. Even in this case, it may not be difficult to infer the shape of  $C_l^{21cm}$  from the shape of  $C_l^{cc}$ .

Our technique is different from standard polynomial-fitting approaches (e.g., McQuinn et al. 2006; Liu et al. 2009). First, although we assume a polynomial dependence of the foregrounds on frequency, we do not need the actual fitting stage. Therefore our technique can be used as a synergistic technique to previous standard suggestions. Second, since  $C_l \propto \sum |T^2|$ , we expect that the high-order frequency dependence of  $T$  may cancel out during the summation. Therefore, in the power spectrum we may have a smoother signal which is much easier to constrain. Third, our technique can give a useful insight for removing noise. Suppose that noise signals are larger than or comparable to the 21-cm signals and that the 21-cm signals at  $\nu$  and  $\nu'$  are correlated if  $|\nu - \nu'| \lesssim \Delta\nu = \nu_{i+1} - \nu_i$ . In this case our technique will give an average spectrum of the noise and the 21-cm signals,  $\sim C_l^{noise} + C_l^{21cm}$ . Now, we add  $M-1$  new channels between each  $\nu_i$  and  $\nu_{i+1}$  ( $i = 1, \dots, N$ ), so that there are a total of  $NM$  channels. Here we assume that the total bandwidth stays roughly the same and the bandwidth of each channel is now  $\sim M$  times narrower than before. Then we apply our technique again. Note that the 21-cm signals are correlated in adjacent channels, while the noise signals are not. The newly obtained average spectrum is now proportional to  $\sim C_l^{noise} + C_l^{21cm} / \sqrt{M}$ . Therefore, by comparing the two results, we may extract the spectrum of the 21-cm signals. For example, if the noise and the 21-cm signals have different dependence on  $l$  (or  $k$ ), we can apply the technique in Cho & Lazarian (2010).

#### 4. SUMMARY

We have described a new technique to remove the foreground from redshifted 21-cm observations. We have assumed that the foreground signals change slowly as the frequency changes: we have assumed up to a quadratic dependence of  $T_{\nu_i}^{for}(u, v)$  on frequency. We obtain the foreground spectrum by simply adding all the observed  $T_{\nu_i}(u, v)$ . If the observations are done in real space, we add all the  $T_{\nu_i}(\theta_x, \theta_y)$  in real space first and then we perform the Fourier transform. When we add  $T_{\nu_i}(u, v)$  of all channels, the foreground spectrum goes up by a factor of  $\sim N^2$  because they are highly correlated. However, the 21-cm spectrum goes up by a factor of  $\sim N$  because the signals in different channels contribute randomly. This way, we can obtain an accurate shape of the foreground power spectrum. Then, we obtain the 21-cm power spectrum by subtracting the foreground power spectrum obtained this way. We have described how to obtain the average 21-cm spectrum (Eqs. [8] and [12]). We have derived the condition for neglecting the cross-correlation term (Eq. [18]).

J.C.’s work was financially supported by the National Research Foundation of Korea (NRF) (2011-0012081). AL acknowledges the support of the NSF Center for Magnetic Self-Organization, the NASA grant NNX11AD32G, and the NSF grant AST 0808118. PT is partly supported

by NSF grant AAG 0908900.

## REFERENCES

- Ansari, R., Le Goff, J., Magneville, C., Moniez, M., Palanque-Delabrouille, N., Rich, J., Ruhlmann-Kleider, V., & Yèche, C. 2008, ArXiv e-prints (0807.3614)
- Ansari, R., et al. 2011, ArXiv e-prints (1108.1474)
- Backer, D. C., et al. 2007, in Bulletin of the American Astronomical Society, Vol. 38, Bulletin of the American Astronomical Society, 967
- Bowman, J. D., Morales, M. F., & Hewitt, J. N. 2009, ApJ, 695, 183
- Chang, T.-C., Pen, U.-L., Peterson, J. B., & McDonald, P. 2008, Phys. Rev. Lett., 100, 091303
- Cho, J., & Lazarian, A. 2002, ApJ, 575, L63
- . 2010, ApJ, 720, 1181
- Ghosh, A., Bharadwaj, S., Ali, S. S., & Chengalur, J. N. 2011, MNRAS, 411, 2426
- Lazarian, A., & Finkbeiner, D. 2003, New Astron. Rev., 47, 1107
- Lazarian, A., & Pogosyan, D. 2012, ApJ, 745, 5
- Liu, A., & Tegmark, M. 2011, Phys. Rev. D, 83, 103006
- Liu, A., Tegmark, M., Bowman, J., Hewitt, J., & Zaldarriaga, M. 2009, MNRAS, 398, 401
- Loeb, A., & Wyithe, J. S. B. 2008, Physical Review Letters, 100, 161301
- Loeb, A., & Zaldarriaga, M. 2004, Physical Review Letters, 92, 211301
- McQuinn, M., Zahn, O., Zaldarriaga, M., Hernquist, L., & Furlanetto, S. R. 2006, ApJ, 653, 815
- Morales, M. F., Bowman, J. D., & Hewitt, J. N. 2006, ApJ, 648, 767
- Morales, M. F., & Hewitt, J. 2004, ApJ, 615, 7
- Morales, M. F., & Wyithe, J. S. B. 2010, ARA&A, 48, 127
- Seo, H.-J., Dodelson, S., Marriner, J., McGinnis, D., Stebbins, A., Stoughton, C., & Vallinotto, A. 2010, ApJ, 721, 164
- White, M., Carlstrom, J. E., Dragovan, M., & Holzappel, W. L. 1999, ApJ, 514, 12
- Wolfe, A., Gawiser, E., & Prochaska, J. X. 2005, Annu. Rev. Astron. Astrophys., 43, 861
- Wyithe, S., Loeb, A., & Geil, P. 2008, MNRAS, 383, 1195
- Zaroubi, S., & Silk, J. 2005, MNRAS, 360, L64